*International Symposium of Research Students on Materials Science and Engineering*
*December 20-22, 2004, Chennai, India*
*Department of Metallurgical and Materials Engineering, Indian Institute of Technology, Madras*

# CONTROL OF ABNORMAL GRAIN GROWTH AND DIELECTRIC PROPERTIES OF FERROELECTRIC STRONTIUM BARIUM NIOBATE

**Pankaj Kumar Patro**
*Department of Metallurgical Engineering and Materials Science*
*Indian Institute of Technology, Bombay*
*Mumbai 400 076, India*

## ABSTRACT

Strontium Barium Niobate (SBN) is a tetragonal tungsten bronze structured ferroelectric material. The unusual sintering behavior of SBN exhibits abnormal grain growth, duplex microstructure and low density that has plagued commercial exploitation of SBN. The formation of duplex microstructure becomes more prominent when synthesized by conventional solid-state approach. Although the exact reason of duplex microstructure is not known, it is believed that composition inhomogeneity is one of the reasons of such ambiguity. Will homogeneous mixing will eliminate this problem? To answer this question, coprecipitation a wet chemical route, has been employed for synthesis of SBN. In coprecipitate route, the precursors are mixed in the molecular level. It is thought that the improved composition uniformity might help in eliminating microstructure related problems with improved dielectric properties. Our findings in this connection on microstructure dielectric and ferroelectric properties are discussed in the manuscript.

## 1. INTRODUCTION

Strontium Barium Niobate ($Sr_xBa_{1-x}Nb_2O_6$, $0.25 \leq x \leq 0.75$, abbreviated as SBN) is a promising lead free ferroelectric-based material, owing to its large pyroelectric[1], electro-optic[2], non-linear optical properties[3] etc. The physical and electrical properties vary with composition and sintering conditions. Although single crystal of SBN with varying composition has been used immensely, it finds restricted application because of its difficulty in fabrication and associated high cost. For optical applications, it is desirable that SBN should have a density near to theoretical one and uniform microstructure. But SBN ceramic, with nearly theoretical density, is difficult to obtain during pressureless sintering because of abnormal grain growth[4]. Efforts have been made to obtain high density SBN by hot pressing[5], double stage sintering[4] and using sintering aids[6]. Alternate synthesis methods such as partial coprecipitation[7], coprecipitation[8], solution combustion[9], sol-gel[10], EDTA-complex chemical route[11] etc. have also been employed to improve its physical, dielectric and microstructural properties.

In this paper, the conventional solid-state synthesis route and coprecipitation method the wet chemical route has been adopted to investigate the effect of precursors on the microstructural and dielectric properties.

## 2. EXPERIMENTAL

The precursors used for synthesis of SBN by solid-state method were $Nb_2O_5$ (99.99%), $Sr(NO_3)_2$(99%) and $Ba(NO_3)_2$(99%), procured from Aldrich, USA. The stoichiometric amount of the pre-dried powder was wet mixed with the help of an automatic agate mortar (Retsch, Germany). Methanol was used as wet mixing agent. This was the further ball milled using

zirconia balls for 24 hrs using methanol as grinding medium. The calcination of the ball milled powder was done at different temperature to obtain the single phase of SBN, which was confirmed of XRD. The phase pure powder was palletized and sintered at different temperatures. The sintered pellets were subjected to microstructural and dielectric characterization. For simplicity the pellets sintered at 1250, 1300 and 1350°C are abbreviated as SN1250, SN1300 and SN1350. The schematic of the synthesis method followed is given in Figure 1(a).

For synthesis of SBN50 by coprecipitation method $Sr(NO_3)_2$ (99%, Aldrich USA), $Ba(NO_3)_2$ (99%, Aldrich USA), $NbCl_5$ (99%, Aldrich USA) and liq. $NH_3$ (Qualigen, India) as precipitant were used. $NbCl_5$ was used as the source of Nb-oxalate. First Liq. $NH_3$ was added to $NbCl_5$, which resulted in the formation of $Nb_2O_5.xH_2O$. Addition of oxalic acid and few drops of $H_2O_2$ facilitated the dissolution of the $Nb_2O_5.xH_2O$ at room temperature by breaking the $Nb_2O_5$ polymer chain resulting in a transparent Nb-oxalate solution[9]. The coprecipitation reaction was carried out by drop wise, slow addition of $Sr(NO_3)_2$ and $Ba(NO_3)_2$ from one burette and Nb-oxalate from another burette to a three necked round bottomed flask containing excess ammonia solution. The precipitation reaction was carried out under continuous stirring condition using a magnetic stirrer. During the reaction the pH, was maintained within10-11. The precipitate was allowed to settle down overnight. No additional precipitation on further addition of aqueous liq. $NH_3$ to the supernatant liquid confirmed the completion of reaction. The precipitate was filtered, washed with water followed by methanol and vacuum dried at room temperature. Then it was calcined at different temperatures and the phase analysis was carried out using X-ray diffraction technique. The phase pure powders are sintered and characterized. The schematic representation of the steps followed to synthesize SBN by coprecipitation is given in the Figure 1(b). For simplicity the samples sintered at 1250, 1300 and 1350°C are abbreviated as CPAH1250, CPAH1300 and CPAH1350.

## 3. RESULTS AND DISCUSSIONS

X-ray diffraction of the calcined powder showed the presence of pure SBN50 ($Sr_{0.5}Ba_{0.5}Nb_2O_6$) phase after the calcination temperature of 1150°C for both the sets of samples. The transmission electron microscopy showed the particle size of the calcined powder (1150°C) having the pure SBN50 phase to be in the range of ~250 nm for the powder synthesized by conventional solid-state route, whereas it was 100-250 nm for coprecipitation method (Figure 2(a and b)). On close observations it could be found that the edges of former have curved edges where as latter has sharp edges. A fair degree of agglomeration was also observed in both the sets.

The Scanning Electron Micrograph of the sintered pellets is shown in Figure 3 (a, b and c) and 4 (a, b and c) for solid-state and coprecipitation based samples corresponding to the sintering temperature of 1250, 1300 and 1350 respectively. The micrograph corresponding to SN1250 (Fig. 3(a)) shows that, it can be seen that, the grains are of the order of 7μm. Figure 3(b), the micrograph corresponding to SN1300 shows two types of grains. One is small in size, elongated grains of the range of 10-15 μm the other type is very large in size ranges between 50-150 μm. This grain seems to very thin and as if transparent in nature so that the presence of smaller grains (of type one) can be seen. Figure 3(c) corresponding to SEM micrograph of SN12350 shows again the presence of duplex microstructure with two types of grain. The smaller grains in the micrograph are more or less rectangular in shape and also show the presence of micro cracks. For this sintering temperature, the bigger grains now have become of order of 200 μm.

Figures 4 (a, b and c) show the Scanning Electron Micrographs of the CPAH1250, CPAH1300 and CPAH1350 samples. The micrographs show uniformity in the grain size. Figure 4(a), corresponding to CPAH1250, shows some pores, showing that the pellet is not very well sintered. Figure 4(b), shows that the sample is well sintered having uniform grains. A very few

number of grains with a tendency of uni-axial grain growth were also seen. A large number of uni-axial micro-rod shaped grains were seen in the case CPAH1350 (Figure 4(c)). This may be due to Ostwald ripening of grains, where the bigger grains grow at the expense of smaller grains. The Image analyses of the micrographs show that the mean grain sizes are 0.70, 0.78 and 3.46 μm and aspect ratios are 1.34, 1.54 and 3.46 for CPAH1250, CPAH1300 and CPAH1350 respectively.

From the above discussion it is clear that there is a striking dissimilarity in the grain morphology when the synthesis approach is different. The former resulted in a duplex microstructure with abnormal grain growth and micro-cracks. The latter resulted in a uniform microstructure with no abnormal grain growth. At the sintering temperature of 1350°C, however some small and elongated grains were observed in the micrographs. This microstructural difference is liked to be reflected on the dielectric and ferroelectric properties which are discussed subsequently.

The dielectric properties of the sintered pellets were measured, from till 200°C, using a high resolution dielectric analyzer with standard internal reference. The measurement was done from 100Hz to 1MHz in the heating cycle.

The porosity corrected dielectric constant[12] vs. temperature plot for poled solid state based and coprecipitation based samples for the sintering temperatures of 1250,1300 and 1350 are shown in Figures 5(a, b and c) and 6(a, b and c) respectively. The broad dielectric peak indicates the second order phase transformation i.e. characteristics of relaxor ferroelectrics. But interestingly, the shift of $T_m$ with frequency is not very prominent for the solid-state based where as it is clearly visible for the coprecipitation based samples.

Figure 5(a), corresponding to SN1250 shows a very low $\varepsilon'_{max}$ value (535). With increase in the sintering temperatures the $\varepsilon'_{max}$ increased to 897 and 1428 for SN1300 and SN1350 respectively. Interestingly $T_m$, the ferroelectric-paraelectric phase transition temperatures were found to be varying with sintering temperature. $T_m$ values were found to be 110, 120 and 130°C for SN1250, SN1300 and SN1350 respectively. The change of $T_m$ with sintering temperature may be dependent upon the stress in the samples. Higher the stress the lower is the $T_m$. In the present cases, the SEM micrographs show that with in crease in sintering temperature, it results in a duplex microstructure with abnormal grain growth and micro-cracks. These micro-cracks helped in releasing the stress due to abnormal grain growth and hence in turn increased $T_m$ values[13].
For CPAH1250, CPAH1300 and CPAH1350, $\varepsilon'_{max}$ were 2717, 2847 and 3281 respectively. Similarly $\varepsilon'_{RT}$ (dielectric constant at room temperature) was 2327, 2779 and 2643 respectively (Figure 6(a, b and c)). Ferroelectric-paraelectric transition temperature (Tm) was found to be 47, 57 and 60 °C for CPAH1250, CPAH1300 and CPAH1350 respectively for the frequency 1KHz.

It can be clearly seen that there is a notable difference in the dielectric properties of Strontium Barium Niobate, when processed through two different routes. SBN, by coprecipitate route resulted in a material with the dielectric properties superior to those synthesized by conventional solid-state route. The room temperature dielectric constants ($T_{RT}$) for the coprecipitation synthesized are significantly higher than the conventionally processed SBN.

The ferroelectric hysteresis loop at an electric field of 15 kV/cm at different frequencies for the samples are shown in the Figures 7 (a, b and c) and 8 (a, b and c) for conventionally and coprecipitation route synthesized SBN respectively. It can be clearly seen that for the solid-state processed sample, the highest polarization was observed for SN1250. However, Ps values decreased with increase in sintering temperatures in samples synthesized by solid-state route.

The decrease in ferroelectric properties can be attributed to the duplex microstructure with abnormal grain growth. The effect of abnormal grain growth which was not of much significance on the dielectric properties played a major role in decreasing the ferroelectric properties of SBN. This can also be noted that, the PE data could not be acquired for 1Hz, because of lossy nature of the material.

For SBN synthesized by coprecipitation route, non-lossy PE loops were obtained (Figure 8 (a, b and c)). For 1 Hz, the maximum saturation polarization observed for CPAH1350 (5.6 $\mu C/cm^2$). Similarly, the saturation polarization ($P_s$) of CPAH1250 and CPAH1300 were 2.93 and 4.03 (for 1 Hz) respectively.

It is quite clear that, SBN by coprecipitate synthesis method resulted in a material with better ferroelectric properties and non-lossy nature.

Some further characterizations show that the SBN by coprecipitate route follows Vogel-Fulcher relationship in turn revealed the dipolar glass nature with freezing temperature $T_f$ ~315K. The leakage current measurement varied from $10^{-5}$ to $10^{-11}$ A during the IV characterization for these materials (15 - 0 kV/cm). Time dependent leakage current was found to be varying between $10^{-6}$ to $10^{-8}$ A when measured at 1000ms "soaking time" and 10000ms "measured time". Only 0.06% in the change in saturation polarization was observed after the electric cycling fatigue of $10^6$ cycles at 15kV/cm. The material followed the "Modified Neel's Law", indicating the presence of non-zero interaction polarization.

## 4. CONCLUSIONS

In conclusion, SBN synthesized by coprecipitation method not only resulted in uniform microstructure with no abnormal grain growth but also remarkably improved the dielectric and ferroelectric properties. It also showed the relaxor behavior, followed V-F relation ship indicating dipolar-glass nature, low time induced as well as field induced leakage current, superior electric fatigue resistance properties and above all $T_m$ value close to room temperature. All this properties makes strontium Barium Niobate synthesized by coprecipitation method a better choice for device applications than the material synthesized by the conventional solid-state approach.

## ACKNOWLEDGEMENTS:

The author acknowledges Sophisticated Analytical Instrument Facility (SAIF), IIT-Bombay for TEM and SEM studies. He also acknowledges CSIR for the Senior Research Fellowship grant.

**REFERENCES:**

[1] Glass, A. M., J. Appl. Phys., 40 (1969) 4699.
[2] Liu, S. T., Maciolek, R. B., Zook, J. D., Rajagopalan, B., Ferroelectrics 87 (1988) 265.
[3] Xu, Y., Chen, H. C., Liu, S. T., Jpn. J. Appl. Phys. 24 (1985) 278.
[4] VanDamme, N. S., Sutherland, A. E., Jones, L., Bridger, K., Winzer, S. R., J. Am. Ceram. Soc., 74 (1991) 1785.

[5] Nagata, K., Yamamoto, Y., Igarashi, H., Okazaki, K., Ferroelectrics, 38 (1981) 853.
[6] Lee, S. I., Choo, W. K., Ferroelectrics, 87 (1988) 209.
[7] Patro, P. K., Kulkarni, A. R., Harendranath, C. S., J. Euro. Cera. Soc., 23 (2003) 1329.
[8] Patro, P. K., Kulkarni, A. R., Harendranath, C. S., Mat. Res. Bull. 38 (2003) 249.

[9] Patro, P. K., Deshmukh, R. D., Kulkarni, A. R., Harendranath, C. S., J. Electroceramics, 13 (2004) 479.

[10] Hirano, S., Yogo, T., Kikuta, K., Ogiso, K., J. Am. Ceram. Soc., 75 (1992) 1697.
[11] Panda, A. B., Pathak, A., Pramanik, P., Mat. Lett., 52 (2002) 180.
[12] Rushman, D. F., Strivens, M. A., Proc. Phys. Soc., 59 (1947) 1011.
[13] Patro, P. K., Kulkarni, A. R., Harendranath, C. S., Ceram. Int. 30(7) (2004) 1405-1409.

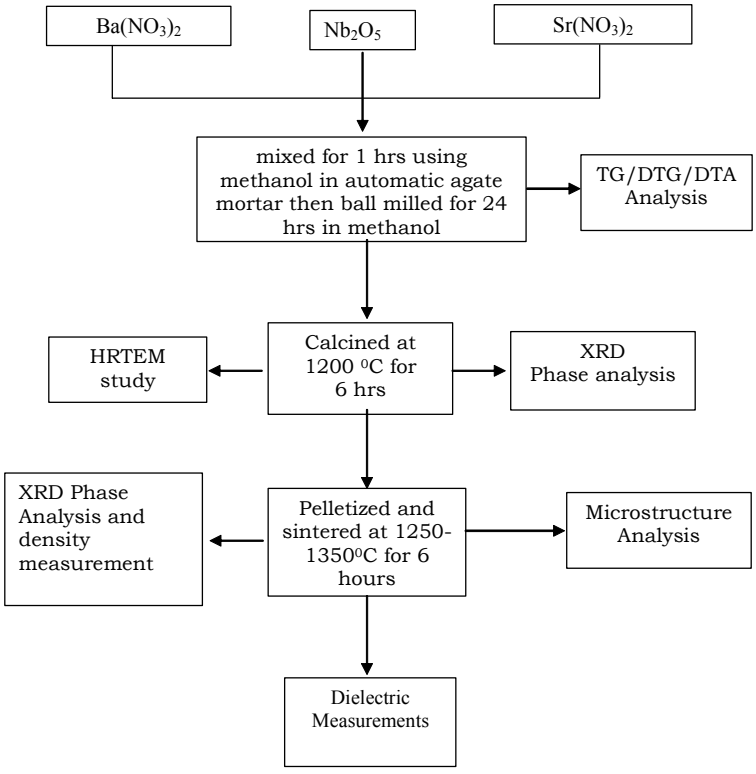


**Fig. 1(a)-: Schematic of the steps followed during conventional solid-state synthesis route.**

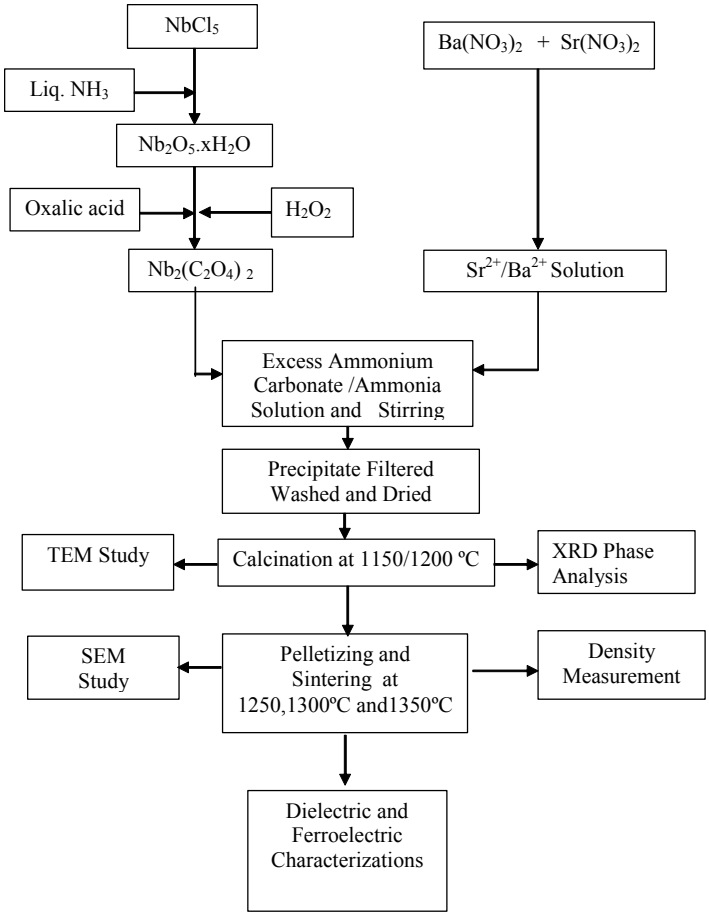


**Fig. 1(b)-: Schematic of the steps followed during coprecipitation synthesis route.**

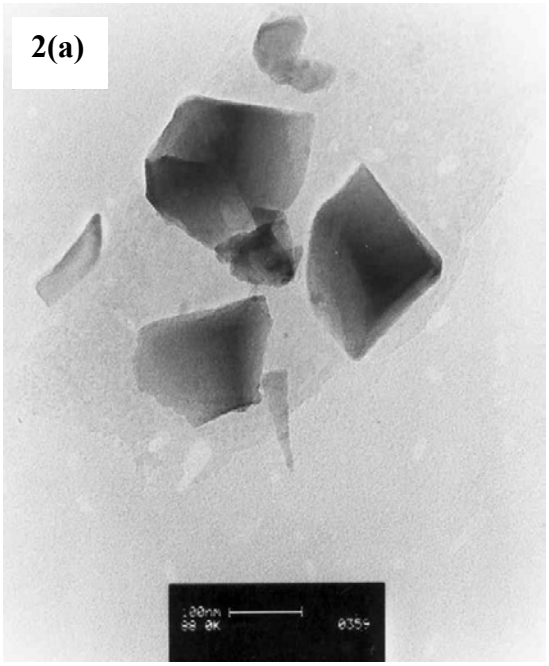


**Fig.2 (a)-: Transmission Electron Micrograph of calcined SBN50 powder synthesized by conventional solid-state route.**

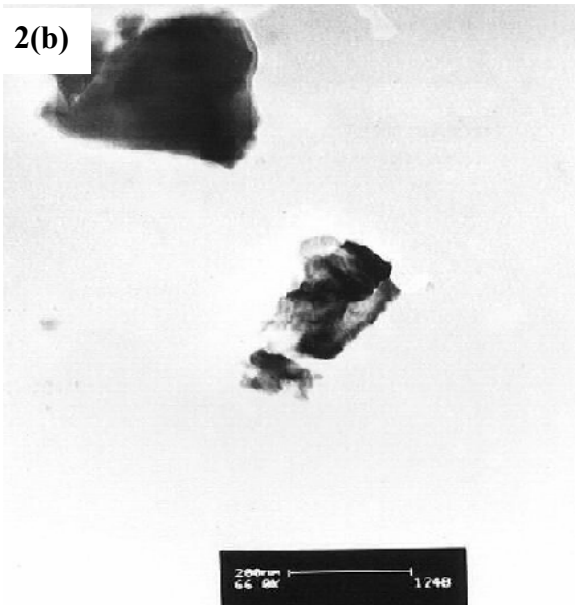


**Fig.2 (b)-: Transmission Electron Micrograph of calcined SBN50 powder synthesized by coprecipitation route**

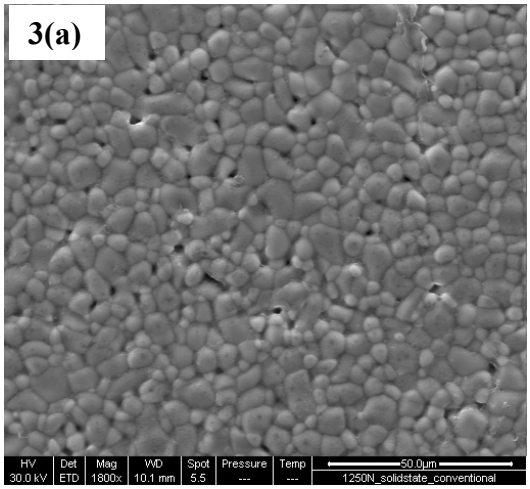


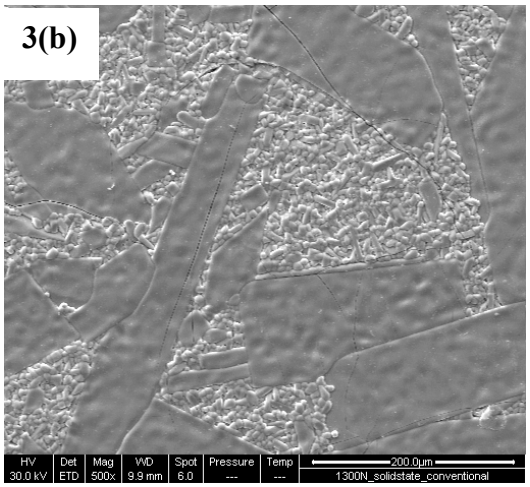


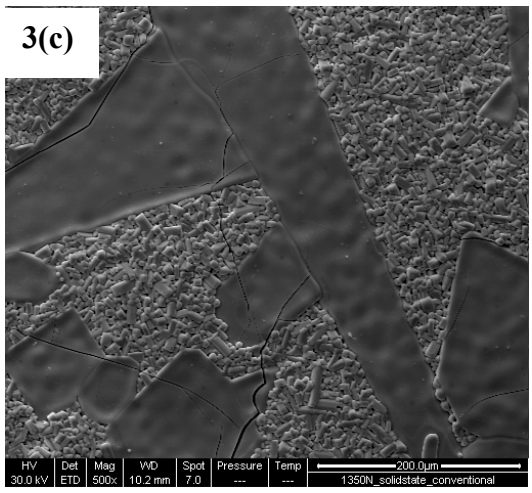


**Fig. 3 -: Scanning Electron Micrograph of sintered pellets of SBN50 synthesized by solid-state route [(a)SN1250, (b)SN1300 and (c)SN1350.**

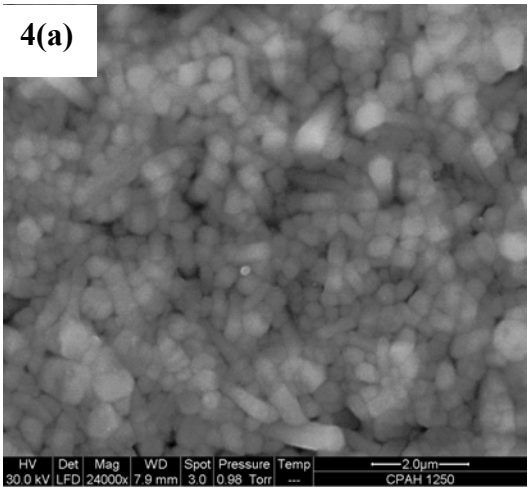


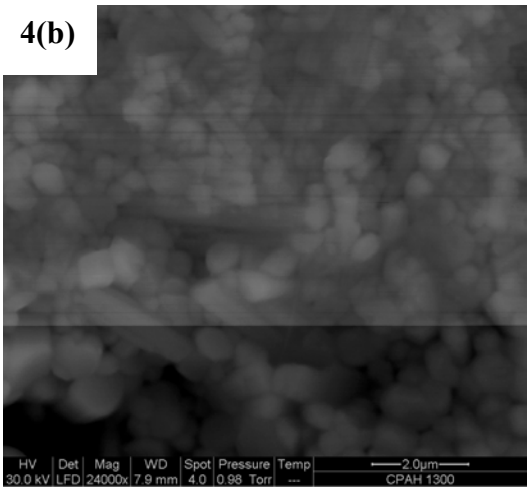


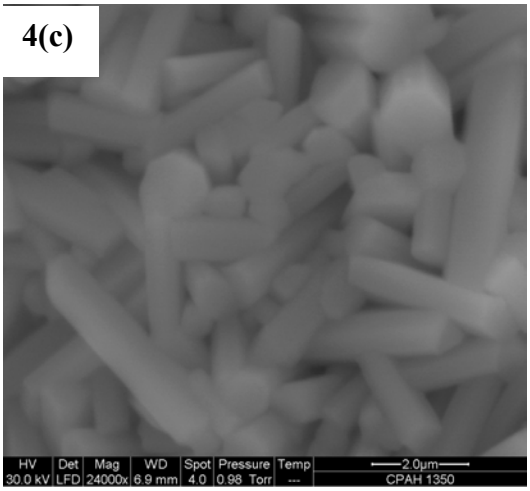


**Fig. 4 -: Scanning Electron Micrograph of sintered pellets of SBN50 synthesized by coprecipitate route. [(a) CPAH1250, (b) CPAH1300 and (c)CPAH1350]**

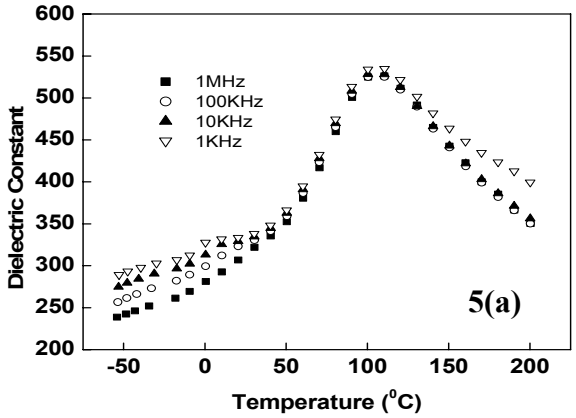


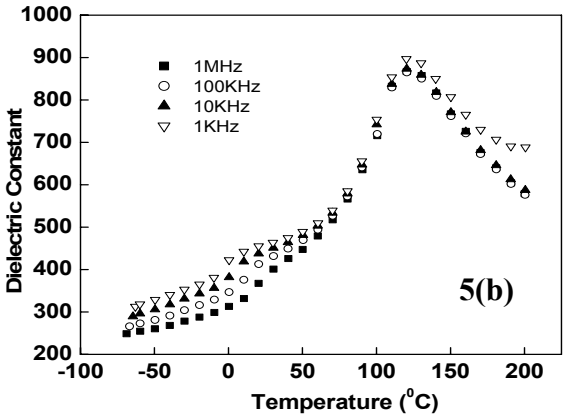


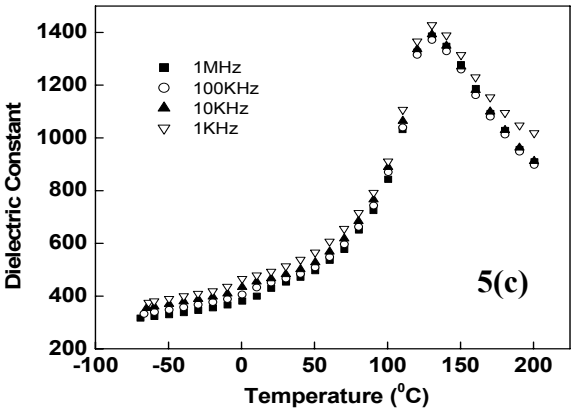


**Fig. 5 -: Variation of Dielectric constant against temperature for sintered pellets of SBN50 synthesized by conventional solid-state route. [(a) SN1250, (b) SN1300 and (c) SN1350]**

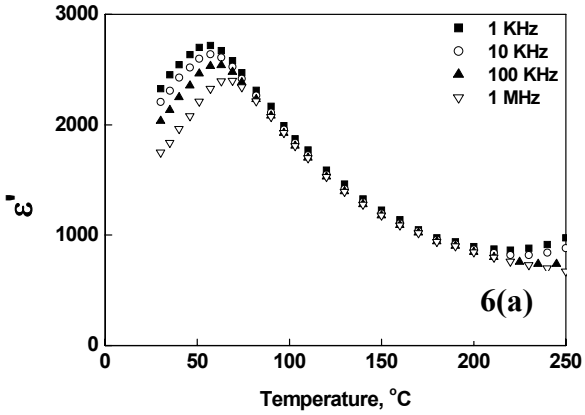


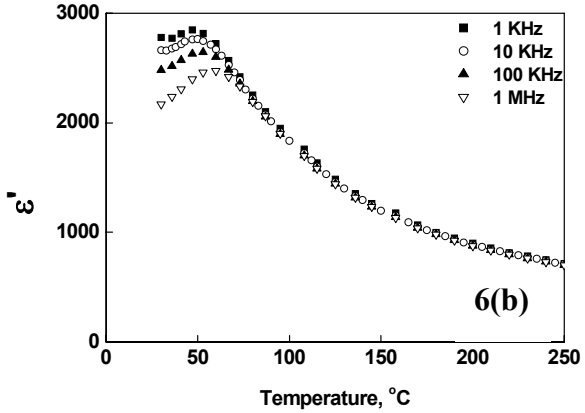


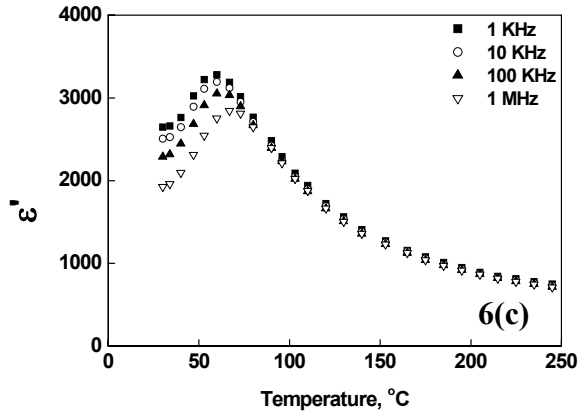


**Fig. 6 -: Variation of Dielectric constant against temperature for sintered pellets of SBN50 synthesized by coprecipitate route. [(a) CPAH1250, (b) CPAH1300 and (c) CPAH1350]**

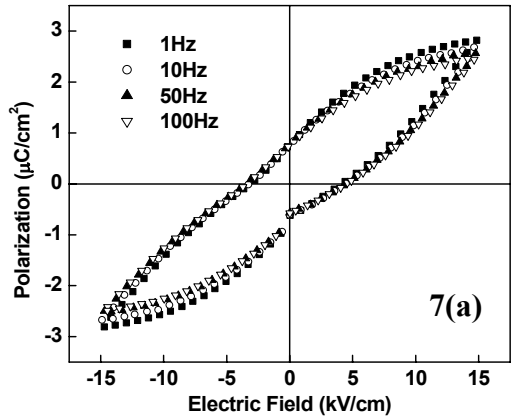


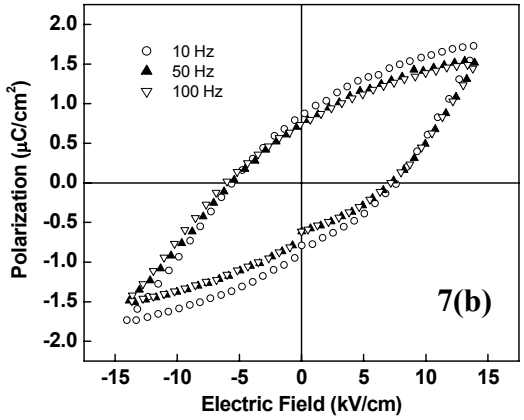


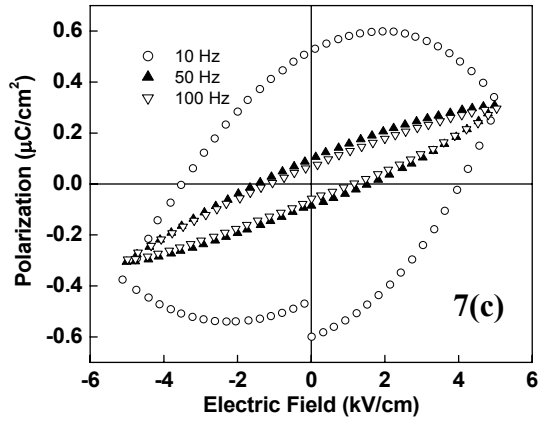


**Fig. 7 -: Ferroelectric Hysteresis loop of SBN50 synthesized by solid-state route [(a) SN1250, (b) SN1300 and (c) SN1350] at different frequencies.**

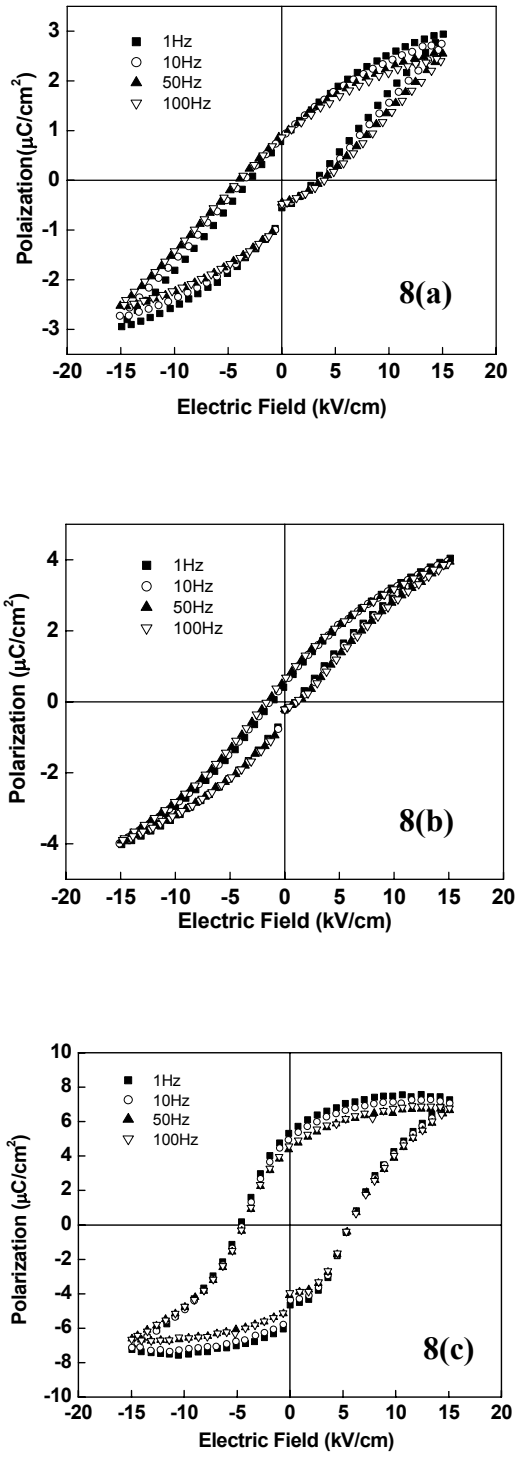


**Fig. 8 -: Ferroelectric Hysteresis loop of SBN50 synthesized by coprecipitate route [(a) CPAH1250, (b) CPAH1300 and (c) CPAH1350] at different frequencies.**